tude of the error voltage, which in turn is proportional to the deviation of the source frequency from f_0. Further, the sense of correction will correspond to the polarity of the error. Note that the frequency pull-in range is not limited to the frequency separation between the peaks of the two cavity responses.

Design Consideration for Cavity Modulation

The design of a microwave resonant cavity which could be cyclically tuned by the application of a periodic voltage to a solid state device suggested the choice of the TM_{011} mode for several reasons. 1) The electric field is normal to the end plates of the cavity. A slight perturbation of this field at the center of the endplate where the electric field is maximum will most effectively detune the cavity. A disk mounted above the center of the endplate (see Fig. 1) provides such an effective method of cavity perturbation. A post supporting the disk to the endplate provides a dc return for the varactor.

The input waveguide is iris coupled to the cavity so as to set up the desired TM_{011} mode. The size of the iris is designed to give approximately 30-db decoupling from a one-watt source. This input level is sufficiently low to give ample output without subjecting the varactor to a large enough RF field to excite self oscillation in the diode.

The output from the cavity is obtained from a crystal detector mounted in an external coaxial mount. It is very lightly loop coupled to the cavity to give adequate output level without causing the cavity frequency to be susceptible to change in crystal characteristic, either through replacement or because of environmental change.

Results and Conclusions

It has been experimentally verified that the cavity is free from multimoding within the design frequency band of 6575 Mc to 6875 Mc. This stands in confirmation of the mode selection and method of excitation previously discussed.

The cavity can be tuned to any given frequency within the above band to within 10 kc. Fig. 3 demonstrates that the frequency separation between the two resonant frequencies is approximately 6 Mc when the applied square wave bias is 5.5 v *pp*. The slight dissimiliarity in the Q of the curves is attributable to the different loading of the cavity by the varactor for two different bias conditions. However, the symmetry of the two curves is close enough to give the symmetrical error curve shown in Fig. 4.

From the discriminator-like error curve, it is seen that the normal output level close to a crossover is approximately 60 mv per Mc with the detector terminated in a low impedance of 300 ohms. Further, measurements show that there is ample error voltage for "pull-in" in an AFC system for frequency shift of source out to ± 12 Mc.

The symmetry of the error curve permits the use of a frequency modulated carrier as the signal source, provided the major portion of the spectral energy of the source is located within the range of symmetry. A severe limiting test has shown that with a single tone frequency modulation, using a modulation frequency of 1.2 Mc and a frequency deviation of 2.5 Mc, the resulting frequency shift in the cavity crossover frequency is only 200 kc. In a microwave communication application, 600 multiplexed voice channels, each considered to be deviated 200 kc rms, gives rise to this same statistical peak deviation of 2.5 Mc; and a klystron source modulated with a white noise equivalent of such a 600-voice channel signal causes no detectable shift in the cavity crossover. This test shows that the linearity of the error curve is adequate for an operating AFC. For a CW source, the symmetry requisite in the error characteristic is of no consideration.

Tests performed to determine the characteristics of the cavity under conditions of a change in ambient temperature from $-20°C$ to $+65°C$ have shown that a frequency stability of better than ± 0.005 per cent is obtainable.

Acknowledgment

The authors acknowledge the contributions of M. P. Younger, mechanical engineer in the area of mechanical design.

A. Farokhrooz
J. B. Linker, Jr.
Communication Products Dept.
General Electric Company
Lynchburg, Va.

Nonlinear Biasing Resistors for Microwave Tunnel-Diode Oscillators*

By using a nonlinear rather than a linear stabilizing resistor in tunnel-diode oscillator and amplifier circuits, the dc power dissipation in the resistor may be reduced by a factor of 3 for typical germanium tunnel diodes, and by a factor of 6 for typical gallium arsenide tunnel diodes. At the same time ac loading by the resistor is reduced. Such nonlinear stabilizing resistors may consist of reverse- or forward-biased heavily doped *pn* junctions.

A typical tunnel-diode microwave oscillator circuit[1] is shown schematically in Fig. 1. In order to bias and stabilize the tunnel diode to an operating point on its negative current-voltage characteristic a biasing resistor R_1 is used. The size of R_1 is a compromise between two conflicting requirements. On the one hand, R_1 should be small enough so that sufficient stabilization of the operating point is obtained. This means that the combined characteristic shown dashed in Fig. 2 of R_1 and the tunnel diode should have a positive slope throughout. On the other hand, R_1 should be as large as possible to minimize the dc power loss in the resistor, measured by the shaded area in Fig. 2.

The purpose of this report is to point out the advantage of using a *nonlinear biasing resistor* with a current-voltage characteristic as indicated by the curve R_2 in Fig. 2 and to show how this can be achieved. Such a nonlinear biasing resistor offers a better compromise between the two conflicting requirements than a linear resistor. Particularly, the power dissipation in the resistor, indicated by the double-crosshatched area in Fig. 2, may be considerably reduced compared to a linear resistor, while still maintaining sufficient stabilization, *i.e.*, a positive slope of the combined characteristic.

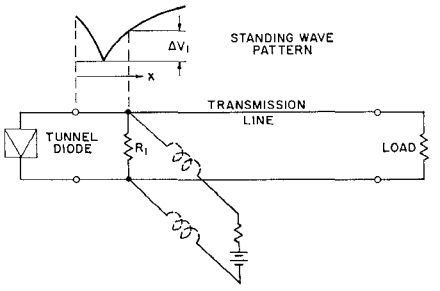

Fig. 1—Schematic picture of biasing arrangement for tunnel-diode oscillator with biasing resistor R_1.

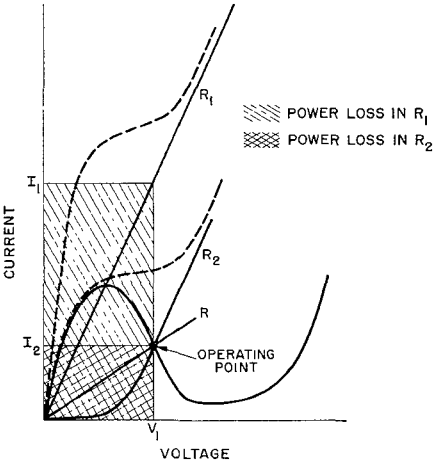

Fig. 2—Current-voltage characteristic of tunnel diode with two alternatives for load resistor. DC power losses for the two alternatives are indicated.

The characteristic of R_2 may be obtained by a *pn* junction in three different ways, namely,

a) a forward-biased diode junction. This has several disadvantages: slow response because of storage of injected minority carriers, either voltage offset if the bandgap is appreciable or very large areas and therefore also high capacitance and poor temperature stability.
b) a forward-biased tunneling junction. This also requires low-bandgap semiconductor material for very low voltage operation as with germanium tunnel diodes. It may be used for gallium arsenide tunnel diodes.
c) a reverse-biased tunneling junction. This is the preferred alternative.

The determination of the reduction in dc power loss is straightforward (see Appendix I). Table I shows the ratio of power loss in a linear biasing resistor P_1 to the power loss in a nonlinear biasing resistor P_2 for tunnel-diode oscillators using germanium

* Received December 26, 1962; revised manuscript received March 6, 1963.
[1] The figures are all lumped.

TABLE I
RELATIVE IMPROVEMENT IN DC POWER LOSS

Tunnel-Diode Oscillator	Relative Improvement P_1/P_2		
	Computed		Measured
	Forward-biased injecting diode at moderate frequencies, case a)	Reverse-biased tunneling junction, case c)	Reverse-biased tunneling junction, case c) (germanium)
Germanium	6	3 5	2.5
Gallium Arsenide	12	6.2	5.5

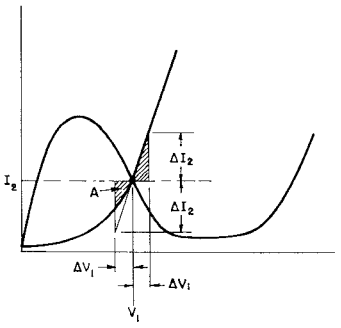

Fig. 3—Current-voltage characteristic of tunnel diode with ac losses indicated.

or gallium arsenide tunnel diodes with a peak current of 50 ma [data by Chynoweth[2] for case c)]. Also shown are results from measurements at 700 Mc for case c). Similar results were obtained at 2000 and 6000 Mc.

A further advantage is offered by the fact that high-frequency loading is somewhat reduced when the location of the stabilizing resistor is not exactly at a voltage node in the standing wave pattern around the oscillator. Again, the reason for this is the nonlinearity. Thus, if voltage exists across the stabilizing resistor, negative voltage swings give less current than with a linear resistor, while positive swings give approximately the same current with both linear and nonlinear resistors. This is illustrated in Fig. 3 where the shaded area A is the reduced power at negative voltage swings. Consequently the high-frequency loading is reduced, and therefore the location of the stabilizing resistor is less critical. (For a quantitative evaluation, see Appendix II.)

APPENDIX I

ANALYSIS OF DC POWER DISSIPATION IN THE BIASING RESISTOR

From Fig. 2

$$R_1 = \frac{V_1}{I_1}. \tag{1}$$

For R_2

$$\left.\frac{dI}{dV}\right|_{V_1} = \frac{1}{R_1}. \tag{2}$$

This insures that for small signals the stabilization is identical in the two cases. The dc power loss P is represented by the shaded areas.

$$\text{For linear resistor} \qquad P_1 = V_1 I_1. \tag{3}$$

$$\text{For nonlinear resistor} \qquad P_2 = V_1 I_2. \tag{4}$$

Combining (1)–(4) we have

$$\frac{P_1}{P_2} = \frac{I_1}{I_2} = \frac{V_1 \left.\frac{dI}{dV}\right|_{V_1}}{I_2} = \frac{R}{R_1} \tag{5}$$

or in words, the improvement is given by the ratio of dc to ac resistance at the operating point (see Fig. 2). In practice the load driven by the oscillator has to be included, modifying the load line R_1. In this simplified argument the load is neglected and open-circuit conditions are assumed.

For a forward-biased pn junction

$$I = I_0(e^{qV/kT} - 1) \approx I_0 e^{qV/kT} \tag{6}$$

$$\frac{dI}{dV} = \frac{q}{kT} I_0 e^{qV/kT} = \frac{q}{kT} I. \tag{7}$$

Then

$$\frac{P_1}{P_2} = \frac{qV_1}{kT}. \tag{8}$$

Values for germanium ($V_1 = 0.17$ v) and gallium arsenide ($V_1 = 0.3$ v) tunnel-diode oscillators are found in Table I. It should be remembered that this could be used only at moderate frequencies because of minority carrier storage (usually <300 Mc).

For a reverse-biased diode[2]

$$\frac{d(\ln I_2)}{d(\ln V_1)} = b + C_1 V_1. \tag{9}$$

For germanium of 0.0035 ohm-cm[3]

$$b \approx 0.8$$

$$C_1 \approx 18.$$

Then

$$I_2 \approx C_2 V_1 e^{bC_1 V_1}. \tag{10}$$

C_2 may be determined from a current-voltage plot such as in Sommers.[4] For a tunnel diode with a peak current of I_p the value of current at the operating point would be $\approx I_p/2$. Then

$$C_2 = \frac{I_p}{2V_1 e^{C_1 V_1}}. \tag{11}$$

C_2 may be evaluated for two typical cases corresponding to a germanium and a gallium arsenide tunnel-diode oscillator. For $I_p = 50$ ma, $V_1 = 0.15$ v (germanium oscillator) and $C_2 = 7.7 \cdot 10^{-3}$. For $I_p = 50$ ma, $V_1 = 0.30$ v (gallium arsenide oscillator) and $C_2 = 3.0 \cdot 10^{-4}$. Now from (5) and (9)

$$\frac{P_1}{P_2} = b + C_1 V_1. \tag{12}$$

Practical values are given in Table I. As can be seen the improvement in dc power is a factor of 3.5 for a typical germanium tunnel-diode oscillator and 6.2 for a typical gallium arsenide tunnel-diode oscillator. Although this improvement is less than for a forward-biased diode, the frequency response is considerably higher, being equal to that of tunnel diodes.

APPENDIX II

ANALYSIS OF AC POWER LOSS IN THE BIASING RESISTOR

Although in principle the stabilizing resistor should be located at a voltage node in the circuit, and therefore not give any ac power loss, in practice some ac power is dissipated in it. This is because the diode is not infinitely small, because the frequency may vary slightly, because its location has not been exactly determined, etc. With a nonlinear stabilizing resistor the ac power losses are reduced and therefore the circuit operation is correspondingly improved. The reduction in ac power losses compared to a linear resistor stems from the fact that the nonlinear resistor draws less current during the negative voltage swings.

To compute the ac power losses, let us assume that the nonlinear load line has the same slope as R_2 at, and above, the operating point. Let us further assume that the voltage swing is $\pm\Delta V_1$ where Δ is a factor <1 and depends on how far from a voltage node the stabilizing resistor is located.

For positive swings the ac power loss is unchanged as the load line is unchanged. For negative swings the ac power loss is represented by the area A as indicated in Fig. 3.

$$P_{AC}' = \frac{\Delta V_1 \Delta I_2}{2} \tag{13}$$

$$P_{AC}'' = \frac{1}{2}\left(\frac{\Delta V_1 \Delta I_2}{2} + A\right) \tag{14}$$

where

$$A = \Delta V_1 I_2 - \int_{(1-\Delta)V_1}^{V_1} \frac{I_p}{2e^{39\ 6V_1}} e^{39\ 6V} dV \tag{15}$$

for the forward-biased diode at room temperature, and

$$A = \Delta V_1 I_2 - \int_{(1-\Delta)V_1}^{V_1} C_2 V^b e^{C_1 V} dV \tag{16}$$

for the reverse-biased tunneling diode. From (13)–(16) the relative improvement P_{AC}'/P_{AC}'' may be determined. In the case of $\Delta = 0.2$, *i.e.*, a voltage swing of $\pm 0.2 V_1$, the improvement is 8–44 per cent as shown in Table II. In practice the improvement may be smaller, but should be noticeable in that the location of the stabilizing resistor should be less critical.

TABLE II
RELATIVE IMPROVEMENT IN AC POWER LOSS FOR $\Delta = 0.2$

Tunnel-Diode Oscillator	P_{AC}'/P_{AC}''	
	Forward-biased injection diode at low frequencies	Reverse-biased tunneling diode
Ge	1 18	1.08
GaAs	1.44	1.16

[2] A. G. Chynoweth, W. L. Feldman, C. A. Lee, R. A. Logan, G. L. Pearson and R. Aigrain, "Internal field emission at narrow silicon and germanium *p-n* junctions," *Phys. Rev.*, vol. 118, p. 425; April, 1960.

[3] *Ibid.*, Fig. 6.

[4] H. S. Sommers, Jr., "Tunnel diodes as high-frequency devices," PROC. IRE, vol. 47, pp. 1201–1206; July, 1959. (See Fig. 1.)

ACKNOWLEDGMENT

Gratefully acknowledged are helpful discussions with H. S. Sommers, Jr., who brought forward the problem of a nonlinear stabilizing resistor, R. M. Williams who suggested the use of reverse-biased junctions, and D. E. Nelson and A. Presser who made experimental tests.

J. T. WALLMARK
RCA Laboratories.
Princeton, N. J.
A. H. DANSKY
RCA Victor Home Instrument Div.
Princeton, N. J.

Mode Cutoff Frequencies in Screened Dielectric Rod Waveguide*

GLOSSARY OF SYMBOLS

$\rho, \phi Z$ = cylindrical coordinates
a = radius of dielectric rod
b = radius of metal screen
$\omega = 2\pi \times$ frequency
μ_r = relative permeability of medium
ϵ_r = relative permittivity of medium
μ_0 = permeability of free space
ϵ_0 = permittivity of free space
$\mu' = \mu_0 \mu_r$
$\epsilon' = \epsilon_0 \epsilon_r$
E, H = electromagnetic field vectors
β = complex component of propagation constant
h = wave number $= (\gamma^2 + \omega^2 \mu' \epsilon')^{1/2}$
λg = wavelength in waveguide
λ = free space wavelength
f = frequency
$J_n(x)$ = Bessel function of first-kind order n
$Y_n(x)$ = Bessel function of second-kind order n
$H_n^{(1)}(x)$ = Bessel function of third-kind order n
$Z_n'(x)$ = first derivative of Bessel function with respect to x

The geometry of the screened dielectric rod waveguide is shown in Fig. 1. The theory for this waveguide has been solved by Beam and Wachowski[1] for the case of $\mu_1 = \mu_2 = 1$. For the general case when $\mu_1 \neq \mu_2 \neq 1$ the characteristic equation becomes

$$n^2 K^2 \beta^2 (q_2 q_4 - q_3 q_6)(q_3 - q_4) + r^4 \omega^2 \mu_0 \epsilon_0 [\{\epsilon_1 q_7 (q_4 - q_3) + \epsilon_2 (q_1 q_3 - q_4 q_5)\} \cdot \{\mu_1 q_7 (q_2 q_4 - q_3 q_6) - \mu_2 (q_2 q_4 q_5 - q_1 q_3 q_6)\}] = 0 \quad (1)$$

where

$$k = \frac{1}{(h_1 b)^2} - \frac{1}{(h_2 b)^2}, \qquad r = \frac{a}{b}$$

$$q_1 = \frac{J_n'(h_2 a)}{h_2 a J_n(h_2 a)}, \qquad q_2 = \frac{J_n'(h_2 b)}{h_2 b J_n(h_2 b)}$$

$$q_3 = \frac{J_n(h_2 a)}{Y_n(h_2 a)}, \qquad q_4 = \frac{J_n(h_2 b)}{Y_n(h_2 b)}$$

$$q_5 = \frac{Y_n'(h_2 a)}{h_2 a Y_n(h_2 a)}, \qquad q_6 = \frac{Y_n'(h_2 b)}{h_2 b Y_n(h_2 b)}$$

$$q_7 = \frac{J_n'(h_1 a)}{h_1 a J_n(h_1 a)}.$$

At cutoff $\beta = 0$ and two equations result:

$$\epsilon_1 q_7 (q_4 - q_3) - \epsilon_2 (q_4 q_5 - q_1 q_3) = 0 \quad (2)$$

$$\mu_1 q_7 (q_2 q_4 - q_3 q_6) - \mu_2 (q_2 q_4 q_5 - q_1 q_3 q_6) = 0. \quad (3)$$

At cutoff $h = 2\pi \sqrt{\mu_r \epsilon_r}/\lambda$.

These two equations can be solved graphically by inserting the required values of ϵ, μ, and λ. Eq. (2) gives the cutoff condition for E-type modes and (3) gives the condition for H-type modes.

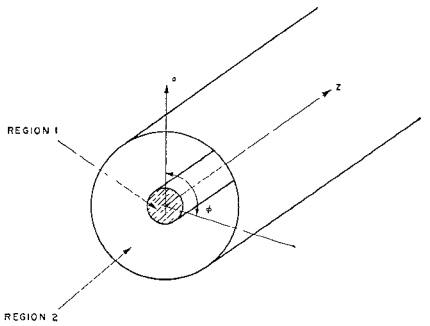

Fig. 1—Waveguide geometry.

TABLE I

Mode	$\frac{b}{c}$	$\frac{b^{(1)}}{c}$
HE_{11}	0.269	0.27
E_{01}	0.305	0.30
HE_{21}	0.477	—
EH_{11}	0.556	—
H_{01}	0.568	0.56

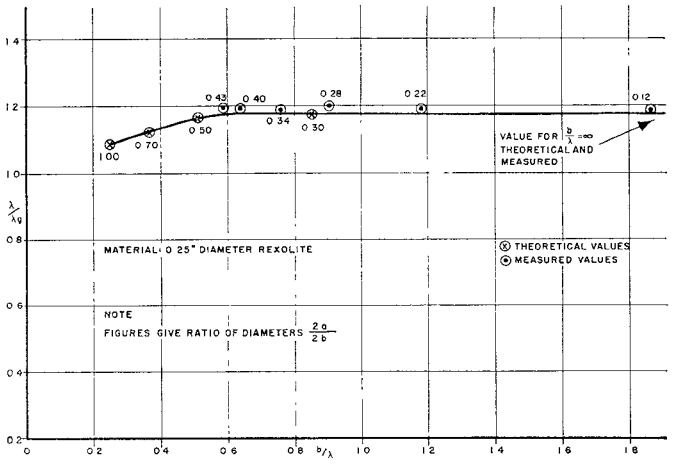

Fig. 2—Theoretical and measured guide wavelengths.

These equations have been solved for the first five modes in a screened dielectric rod waveguide for $\epsilon_1 = 2.5$ and $r = 0.3$. Values of b/λ_c are given in Table I where they are compared with the graphical values of Beam and Wachowski. The mode nomenclature gives the order of the Bessel function and the order of the root of (2) or (3). The mode has been termed HE if solved by (3) for $n \neq 0$ and EH if solved by (2) for $n \neq 0$.

It can be seen that the dielectric rod reduces the cutoff frequency of the EH_{11} mode so that the E_{11} limit mode and the H_{01} mode no longer have coincident cutoff frequencies. It is also interesting to note that the effect of the dielectric rod of $r = 0.3$ on the H_{21} mode is very small. (For the H_{21} mode $b/\lambda_c = 0.486$.) This is consistent with the mode pattern of the H_{21} mode.

Some measurements of the HE_{11} mode wavelength in a screened dielectric rod waveguide have been made for 0.25-in rexolite rod ($\epsilon_r = 2.5$) at 24,000 Mc. Fig. 2 shows that above a particular value of b/λ

* Received January 7, 1963; revised manuscript received March 18, 1963.

[1] R. E. Beam and H. M. Wachowski, "Shielded Dielectric Rod Waveguide," Microwave Lab., Northwestern University, Chicago, Ill., pp. 270–309; 1950 (Final rept. on investigation of multimode propagation in waveguides and microwave optics.)